

News & Views

Does Nitric Oxide Contribute to Progressive Cardiac Tissue Damage and Dysfunction After Infarction?

CORINNE BERTHONNECHE,¹ MARIE-CLAIRE TOUFEKTSIAN,¹ STÉPHANE TANGUY,²
CATHERINE GHEZZI,³ JOËL DE LEIRIS,¹ and FRANÇOIS BOUCHER¹

ABSTRACT

Myocardial infarction induces contractile dysfunction and remodeling that can lead to heart failure. Nitric oxide has been proposed as one of the major actors of this pathophysiologic process. We note that *N*^G-nitro-L-arginine methyl ester (L-NAME) administration from day 2 to day 7 after myocardial infarction in rats improves stroke volume, preserves cardiac compliance, and reduces infarct expansion. Our observations lead to the hypothesis that the mechanisms by which cytokines contribute to myocardial remodeling and dysfunction in the days after infarction might involve •NO signalling pathways. *Antioxid. Redox Signal.* 9, 757–763.

•NO PRODUCTION AFTER MYOCARDIAL INFARCTION

SEVERAL LINES OF EVIDENCE support the concept that inflammatory cytokines play a central pathophysiologic role in heart failure (HF). Elevated circulating and myocardial levels of tumor necrosis factor (TNF)- α have been reported in patients with HF (17, 24), with plasma levels correlating with the severity of the disease (6). Furthermore, TNF- α induces biologic effects similar to the phenotypic changes of HF, including contractile depression (8, 27), myocyte growth (26), and induction of a fetal gene program, myocyte apoptosis (16), and extracellular matrix alterations (19). However, the mechanisms of cytokine-induced myocardial dysfunction have not been clearly elucidated and might be both dependent on (8) and independent (27) of •NO.

•NO AND POSTINFARCT CARDIAC COMPLIANCE

To evaluate the role that •NO could play in the myocardium during the days after ischemia/reperfusion, we assessed the effects of early short-term (from day 2 to day 7

after surgery) NOS blockade [by using the nonselective NOS inhibitor *N*^G-nitro-L-arginine methyl ester (L-NAME)] on passive cardiac compliance 7 days after left coronary artery ligation in rats. The complete passive pressure–volume curves of left ventricles of sham-operated animals and rats with myocardial infarction (MI) treated or not with L-NAME show a significant rightward shift of the MI–Control curve *versus* Sham–Control (Fig. 1A), indicating an increase in left ventricular volumes. The MI–L-NAME curve was significantly shifted toward smaller volumes, compared with MI–Controls, at transmural pressures of 0 and 5 mm Hg ($p < 0.05$). Finally, the operating left ventricular end-diastolic volume was significantly less increased in MI–L-NAME compared with MI–Controls (Fig. 1B), suggesting that L-NAME might prevent left ventricular dilation.

•NO AND CARDIAC GEOMETRY

Infarct size was similar among rats that underwent coronary artery ligation (MI–L-NAME: $54 \pm 2\%$ and MI–Control: $57 \pm 2\%$) (Table 1). L-NAME treatment significantly increased the thickness of the interventricular septum 7 days after coronary ligation, whereas the thickness of the

¹Laboratoire TIMC-PRETA, UMR5525, IFRT 130, Université Joseph Fourier, Grenoble, France.

²Laboratoire de Physiologie des Adaptations Cardiovasculaires à l'Exercice (UPRES JE 2426, Université d'Avignon, France.

³Radiopharmaceutiques Biocliniques, INSERM U877, IFRT 130, Université Joseph Fourier, Grenoble, France.

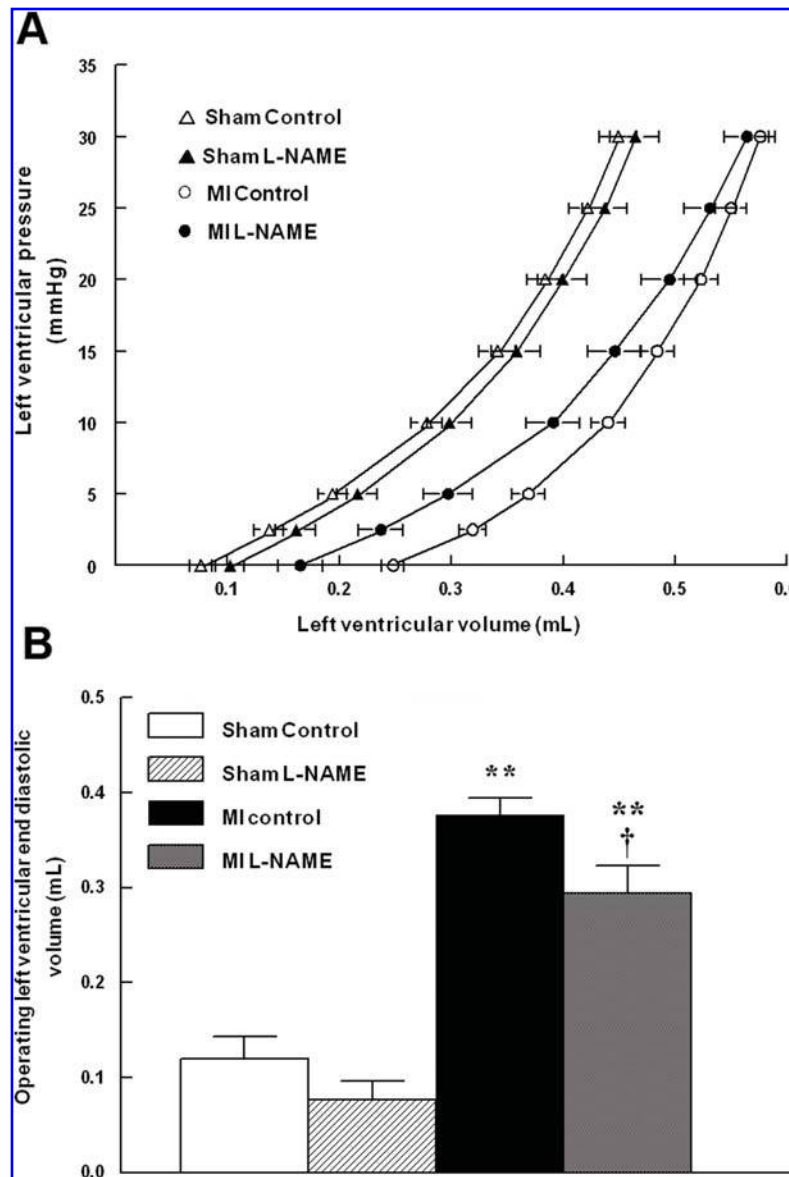


FIG. 1. Left ventricular volume after potassium arrest, measured *ex vivo* during saline infusion over the pressure range 0–30 mm Hg (A). Operating left ventricular end-diastolic volume assessed in sham-operated and ligated rats 7 days after MI (B). Results are expressed as mean \pm SEM. * $p < 0.05$ versus the corresponding sham-operated group. † $p < 0.05$ versus MI-Control, Fisher's PLSD test.

right ventricular free wall remained equivalent in both groups. The thinning of the infarcted wall was significantly reduced in MI-L-NAME compared with MI-Control.

The cavity dilation index (DI) and the thinning index (TI) were statistically equivalent in all rats that underwent coronary artery ligation whether treated with L-NAME or not. Finally, the expansion index (EI), which reflects both the thinning of the infarcted wall and the dilation index of the cavities, was significantly reduced in MI rats treated with L-NAME.

•NO AND CARDIAC FUNCTION

Basal conditions

L-NAME induced a significant reduction in heart rate (HR) in Sham operated rats (Table 2). HR, left ventricular

end-diastolic pressure (LVEDP), and the first derivative of minimal developed pressure (dP/dt_{min}) were similarly affected in both MI groups compared with Sham. Under basal conditions, mean arterial pressure (MAP), left ventricular systolic pressure (LVSP), and the first derivative of maximal developed pressure (dP/dt_{max}) were significantly improved in the MI-L-NAME group compared with MI-Control. Furthermore, in MI rats, L-NAME treatment was associated with a significant improvement of mean abdominal aortic blood flow (A_{Ao}) and stroke volume (SV).

Volume overload

In sham-operated animals, MAP and LVSP were significantly increased in L-NAME-treated rats compared with controls ($p < 0.01$) (Table 3). Again, A_{Ao} and SV were

TABLE 1. EFFECT OF L-NAME ON MORPHOMETRIC VARIABLES CALCULATED FROM TISSUE SURFACES MEASURED ON CROSS SECTIONS OF LIGATED (MI) AND SHAM-OPERATED (SHAM) RAT HEARTS ON DAY 7 AFTER MI

	<i>Experimental groups</i>			
	<i>Sham-control</i> (<i>n</i> = 13)	<i>Sham L-NAME</i> (<i>n</i> = 6)	<i>MI-control</i> (<i>n</i> = 24)	<i>MI-L-NAME</i> (<i>n</i> = 12)
ST (mm)	1.70 ± 0.07	2.00 ± 0.13	1.74 ± 0.11	2.13 ± 0.12 ^c
RVT (mm)	1.01 ± 0.05	1.11 ± 0.08	1.10 ± 0.06	1.18 ± 0.06
LVT (mm)	1.61 ± 0.06	1.58 ± 0.17	0.44 ± 0.03 ^b	0.63 ± 0.02 ^{bc}
DI	0.32 ± 0.02	0.36 ± 0.05	0.53 ± 0.02 ^b	0.48 ± 0.01 ^a
TI	0.96 ± 0.04	0.79 ± 0.05 ^b	0.26 ± 0.02 ^b	0.30 ± 0.02 ^b
EI	0.33 ± 0.02	0.48 ± 0.09	2.15 ± 0.16 ^b	1.64 ± 0.09 ^{bc}

ST, septal thickness (mm); RVT, right ventricular thickness (mm); LVT, left ventricular thickness (mm); DI, dilation index; TI, thinning index; EI, expansion index.

Results are expressed as mean ± SEM.

^a*p* ≤ 0.05, ^b*p* ≤ 0.01 vs. sham.

^c*p* ≤ 0.01 MI-L-NAME vs. MI-control.

significantly improved in MI-L-NAME-treated group compared with the MI-Control group (*p* < 0.01) after volume overload.

CONCLUSIONS AND OPEN QUESTIONS

Results here reported show that hemodynamic variables, assessed 7 days after MI, are less severely altered in L-NAME-treated animals than in controls. Moreover, abdominal

aortic blood flow and stroke volume are significantly protected by the treatment.

After MI, the impaired myocardium is progressively replaced by a noncontractile fibrous scar, and the remaining undamaged part of the heart adapts to preserve cardiac output with changes in shape and hypertrophy. Although initially beneficial to the heart, cardiac remodeling most often leads to a slow alteration in cardiac function; which results in turn in congestive heart failure (CHF) and increased mortality. Among the different factors that could be responsible for the transition

TABLE 2. EFFECT OF L-NAME ON HEMODYNAMIC VARIABLES ASSESSED AT BASELINE IN LIGATED (MI) AND SHAM-OPERATED (SHAM) RATS 7 DAYS AFTER MI

	<i>Experimental groups</i>			
	<i>Sham-control</i> (<i>n</i> = 14)	<i>Sham-L-NAME</i> (<i>n</i> = 6)	<i>MI-control</i> (<i>n</i> = 18)	<i>MI-L-NAME</i> (<i>n</i> = 9)
HR (beats/min)	434 ± 10 (<i>n</i> = 14)	371 ± 9 ^b (<i>n</i> = 6)	396 ± 8 ^b (<i>n</i> = 15)	370 ± 13 (<i>n</i> = 8)
MAP (mm Hg)	115 ± 5 (<i>n</i> = 14)	133 ± 19 (<i>n</i> = 6)	91 ± 4 ^a (<i>n</i> = 18)	120 ± 12 ^c (<i>n</i> = 9)
LVSP (mm Hg)	150 ± 6 (<i>n</i> = 14)	162 ± 18 (<i>n</i> = 6)	116 ± 5 ^b (<i>n</i> = 18)	147 ± 18 ^c (<i>n</i> = 8)
LVEDP (mm Hg)	0.8 ± 0.9 (<i>n</i> = 14)	0.1 ± 0.8 (<i>n</i> = 6)	6.6 ± 1.3 ^b (<i>n</i> = 18)	5.2 ± 1.6 ^a (<i>n</i> = 7)
dP/dt (×1,000 mm Hg/s)	6.2 ± 0.2 (<i>n</i> = 14)	6.3 ± 0.6 (<i>n</i> = 6)	4.4 ± 0.2 ^b (<i>n</i> = 17)	5.4 ± 0.4 ^c (<i>n</i> = 8)
dP/dt _{min} (×1,000 mm Hg/s)	-5.6 ± 0.3 (<i>n</i> = 14)	-5.8 ± 0.7 (<i>n</i> = 6)	-3.6 ± 0.2 ^b (<i>n</i> = 18)	-4.3 ± 0.4 ^b (<i>n</i> = 7)
A _{Ao} (ml/min)	33.7 ± 3.8 (<i>n</i> = 8)	30.6 ± 3.9 (<i>n</i> = 5)	21.9 ± 1.5 ^b (<i>n</i> = 12)	36.6 ± 4.0 ^d (<i>n</i> = 5)
SV (μl/beat)	81 ± 11 (<i>n</i> = 8)	83 ± 10 (<i>n</i> = 5)	55 ± 3 ^a (<i>n</i> = 12)	98 ± 12 ^d (<i>n</i> = 5)

HR, heart rate (beats/min); MAP, mean arterial pressure (mm Hg); LVSP, left ventricular systolic pressure (mm Hg); LVEDP, left ventricular end-diastolic pressure (mm Hg); dP/dt, maximal (max) and minimal (min) first derivatives of left ventricular developed pressure (mm Hg/s); A_{Ao}, abdominal aortic blood flow (ml/min); SV, stroke volume (μl/beat).

Results are expressed as mean ± SEM.

^a*p* < 0.05, ^b*p* < 0.01 MI vs. corresponding sham.

^c*p* < 0.05, ^d*p* < 0.01 MI-L-NAME vs. MI-control, Fisher's PLSD test.

TABLE 3. EFFECT OF L-NAME ON HEMODYNAMIC VARIABLES ASSESSED AFTER A 1-MIN INFUSION OF RINGER'S SOLUTION (17 ML/KG) IN LIGATED (MI) AND SHAM-OPERATED (SHAM) RATS 7 DAYS AFTER MI

	<i>Experimental groups</i>			
	<i>Sham-control</i>	<i>Sham-L-NAME</i>	<i>MI-control</i>	<i>MI-L-NAME</i>
HR (beats/min)	426 ± 9 (n = 14)	365 ± 14 ^a (n = 6)	365 ± 9 ^a (n = 15)	346 ± 12 (n = 8)
MAP (mm Hg)	146 ± 5 (n = 14)	182 ± 11 ^a (n = 6)	109 ± 3 ^a (n = 18)	124 ± 8 ^a (n = 9)
LVSP (mm Hg)	183 ± 7 (n = 14)	218 ± 12 ^a (n = 6)	132 ± 4 ^a (n = 18)	145 ± 11 ^a (n = 8)
LVEDP (mm Hg)	9.1 ± 1.8 (n = 14)	14.8 ± 3.2 (n = 6)	29.7 ± 1.5 ^a (n = 18)	31.9 ± 1.4 ^a (n = 7)
dP/dt _{max} (×1,000 mm Hg/s)	6.9 ± 0.2 (n = 14)	7.5 ± 0.5 (n = 6)	4.2 ± 0.1 ^a (n = 17)	4.5 ± 0.3 ^a (n = 8)
dP/dt _{min} (×1,000 mm Hg/s)	-6.7 ± 0.2 (n = 14)	-7.2 ± 0.4 (n = 6)	-3.8 ± 0.2 ^a (n = 18)	-4.1 ± 0.3 ^a (n = 7)
A _{Ao} (ml/min)	62.3 ± 6.8 (n = 8)	57.2 ± 2.2 (n = 5)	36.4 ± 2.2 ^a (n = 12)	53.7 ± 2.5 ^b (n = 5)
SV (μl/beat)	151 ± 17 (n = 8)	159 ± 11 (n = 5)	98 ± 6 ^a (n = 12)	157 ± 12 ^b (n = 5)

HR, heart rate (beats/min); MAP, mean arterial pressure (mm Hg); LVSP, left ventricular systolic pressure (mm Hg); LVEDP, left ventricular end-diastolic pressure (mm Hg); dP/dt, maximal (max) and minimal (min) first derivatives of left ventricular developed pressure (mm Hg/s); A_{Ao}, abdominal aortic blood flow (ml/min); SV, stroke volume (μl/beat).

Results are expressed as mean ± SEM.

^a*p* ≤ 0.01; MI vs. corresponding sham.

^b*p* ≤ 0.01 MI-L-NAME vs. MI-control; Fisher's PLSD test.

from adaptive to deleterious cardiac remodeling, nitric oxide (•NO) seems to play a crucial role.

Previous basic and clinical studies have shown that excessive amounts of •NO produced by local induction of NOS₂ (iNOS) may be cardiotoxic by altering myocardial contractility (4, 15) and promoting apoptosis (14). Because TNF-α is a potent inducer of NOS2 (12), it has been postulated that negative inotropic effects of TNF-α may be mediated by enhanced production of •NO in the myocardium. However, conflicting results have been reported regarding the effects of NOS inhibition on cytokine-induced cardiac dysfunction (8, 18, 20, 27).

In a previous study, we showed that 7 days after MI in rats, cardiac function is dramatically affected and well correlated with a myocardial peak of TNF-α and that this time of the follow-up might be of major importance in the development of subsequent HF (1). Moreover, we recently demonstrated that a single intravenous injection of soluble TNF-α receptor type II (sTNF-RII) led to marked cardioprotective effects consisting of improvement in left ventricular end diastolic pressure, significant shift of the pressure-volume curve, and significant improvement in the infarct expansion index (1, 2).

Therefore, it can be hypothesized that the mechanisms by which TNF-α contributes to myocardial remodeling and contractile dysfunction early after MI in rats might involve •NO signalling pathways.

In the heart, •NO has a large variety of targets and can regulate the function of many cardiac cell types as well as cardiac loading. In mammals, •NO is synthesized by three

different isozymes of an enzyme called •NO synthase (NOS). In the heart, all three isozymes of NOS are expressed because numerous different cell types are represented in this organ. Two isozymes, initially identified in the nervous system (nNOS or NOS1) and endothelial cells (eNOS or NOS3), are generally constitutively expressed and are activated by calcium and calmodulin. The third isozyme, generally referred to as the inducible NOS (iNOS or NOS2), is constitutively present at low levels in most cell types under physiologic conditions and is overexpressed after exposure of the cells to cytokines or endotoxins (3). The cellular localization of NOS is specific for each isozyme, allowing the cell to control simultaneously several •NO-dependent signaling pathways.

The aim of this study was to reduce the overall amount of •NO in the myocardium, 7 days after infarction (*i.e.*, at the time of the transient TNF-α overexpression). To achieve this, we chose to use L-NAME, a nonselective inhibitor of NOSs, rather than a selective inhibitor of a given isozyme of the enzyme.

•NO AND CARDIAC GEOMETRY

Our study shows that L-NAME treatment significantly reduces infarct thinning as well as the EI, despite increased afterload. It has been reported that low concentrations of •NO can directly inhibit cardiac myocyte hypertrophy (13), decrease matrix production by cardiac fibroblasts (11), and

promote angiogenesis (5); all of which could beneficially affect ventricular remodeling and contractile function (3). In contrast, higher concentrations of •NO depress myocyte shortening and promote apoptosis; which can, in turn, alter cardiac remodeling (25). In our study, the reduction of the overall •NO production due to the nonselective inhibition of NOSs early after MI might explain the beneficial effects of L-NAME on cardiac geometry.

NOS2 and cardiac dysfunction

Several studies have confirmed the deleterious effects of NOS2 in postinfarct cardiac dysfunction (21). Feng *et al.* (7) showed that increased NOS2 expression contributes to cardiac dysfunction and increases mortality after MI in mice. Moreover, a recent study by Zheng *et al.* (28) demonstrated that NOS2 selective inhibition by *S*-methyl-thiourea (SMT) improves heart function after MI in rats. The improvement of cardiac function by L-NAME treatment in our study might therefore mainly result from the inhibition of NOS2 and the resulting limitation of •NO production. However, the use of a specific NOS2 inhibitor will now be required to verify this hypothesis.

NOS2 and proinflammatory cytokines

In patients with dilated cardiomyopathy, systemic TNF- α and •NO production are proportional to the severity of HF (22). Moreover, several studies have shown a close correlation of TNF- α with systemic and local •NO production (21, 22). Because TNF- α is a potent inducer of NOS2 expression (12), it has been suggested that the negative inotropic effects of TNF- α might result from increased •NO production in the myocardium. The study by Funakoshi *et al.* (10), showing that induction of NOS2 plays an important role in the pathogenesis of cardiac dysfunction in a model of mice overexpressing TNF- α , reinforces this hypothesis. Therefore, we suggest that the cardioprotective effects of L-NAME administered during the transient overexpression of TNF- α after myocardial infarction in rats, might be due, at least in part, to the inhibition of TNF- α -induced •NO overproduction.

CONCLUSION

The improvements of cardiac function and remodeling that are observed in our experimental conditions after L-NAME treatment might be due to the inhibition of the effects of TNF- α or other pro-inflammatory cytokines on the NOS2 pathway. To confirm this hypothesis and further to explore these mechanisms, a selective inhibitor of NOS2 will be tested. Finally, the impact of TNF- α inhibition on the myocardial overexpression of NOS2 and the resulting production of •NO after MI will have to be investigated.

Further elucidation of the cellular signaling pathways involved in the transition of the myocardium from adaptation to dysfunction and heart failure after MI is necessary.

ABBREVIATIONS

A_{Ao}, abdominal aortic blood flow; DI, dilation index; dP/dt, maximal positive (max) and negative (min) first derivatives of left ventricular developed pressure; EI, expansion index; HF, heart failure; HR, heart rate; L-NAME, N^G-nitro-L-arginine methyl ester; LV cav csa, cross-sectional area of the left ventricular cavity; LV csa, cross sectional area of the entire left ventricle; LVEDP, left ventricular end-diastolic pressure; LVSP, left ventricular systolic pressure; LVT, left ventricular thickness; MAP, mean arterial blood pressure; MI, myocardial infarction; RVT, right ventricular thickness; SEM, standard error of the mean; ST, septal thickness; SV, stroke volume; TI, thinning index.

APPENDIX

Notes

1. Materials and Methods

Experiments were performed on adult male Wistar rats (280–320 g body weight), purchased from IFFA CREDO (Lyon, France) and maintained on a standard diet. All experiments were in conformity with the “Guide for the Care and Use of Laboratory Animals” (License number 380436).

All chemicals used in this study were from Sigma (St Louis, MO).

2. Myocardial infarction

After being anaesthetised with an i.m. injection (0.1 ml/100 g body weight) ketamine and xylazine mixture (50 and 10 mg/kg), rats were intubated and ventilated via a tracheal cannula by a constant-volume ventilator (Apelex; rate, 70/min, 0.1 ml/kg). A left thoracotomy was performed at the fourth intercostal space, and the heart was exteriorized by digital pressure on the chest wall. The left coronary artery was ligated 1–2 mm from its origin with a 5-0 silk suture (Autosuture, France). The heart was then quickly returned to the chest cavity, and the chest was compressed to remove any air before being hermetically sealed. To ensure uniformity of infarct, only hearts with an infarct $\geq 40\%$ of the midwall circumference, which were identified and measured by morphometric method, were included in the final analysis. The overall mortality of this model was 25%. The same procedure was followed for sham-operated control animals, but the coronary ligation was untied. No mortality was observed in these sham groups.

3. Experimental design

After surgery, rats were housed in polyethylene cages (three rats per cage), fed a standard laboratory diet, had free access to tap water, and were subsequently studied after 7 days of permanent coronary artery ligation. The animals were randomly assigned ($n = 6$ to 15 per group) to the four experimental groups:

MI-L-NAME: Infarcted animals receiving 10 mg/kg L-NAME per day in drinking water from day 2 to day 7 after MI;

Sham-L-NAME: Sham-operated animals receiving 10 mg/kg L-NAME per day in drinking water from day 2 to day 7 after MI;

MI-Control: Infarcted animals receiving normal tap water from day 2 to day 7 after surgery;

Sham-Control: Sham-operated animals receiving normal tap water from day 2 to day 7 after surgery.

4. In vivo measurement of cardiac function

Hemodynamic studies were performed 7 days after coronary ligation or sham operation. Animals were anesthetized with sodium

pentobarbital (60 mg/kg, 1 ml/kg, i.p.). After tracheotomy, rats were immediately ventilated, and heparin was injected via a saphenous vein (400 IU/kg, i.v.). Body temperature was kept constant at 37°C with a heating blanket controlled by a thermostat and connected to a rectal thermocouple (Homeothermic Blanket System; Harvard Apparatus, Edenbridge, U.K.). A polyethylene catheter, PE 10, was inserted into the right femoral vein to deliver a continuous infusion (6 μ L/min/kg) of sodium pentobarbital, and the left femoral vein also was catheterized to allow volumic overload with thermostated Ringer's solution. Mean arterial blood pressure (MAP) was measured via a PE 50 arterial catheter (left carotid) connected to a pressure transducer (Statham P23XL; Hugo Sachs Elektronik, Hungsten, Germany), and a SRP-407 Millar Mikro Tip catheter (Houston, TX) was inserted into the left ventricle via the right carotid artery to monitor left ventricular systolic (LVSP) and diastolic (LVEDP) pressures and heart rate (HR), and to calculate maximal positive and negative first derivatives of developed pressure (dp/dt_{\max} and dp/dt_{\min}). The rat was then positioned in lateral decubitus, and the abdomen was opened. The abdominal aorta was isolated, and a calibrated flow probe (1.5 or 2 mm i.d.) (Electromagnetic Blood Flow, MDL 1401, Skalar Ltd, Delft, the Netherlands) was placed around the vessel, and mean abdominal aortic blood flow was electromagnetically monitored.

After baseline measurements had been carried out over a 10-min period to reach a steady state, thermostated Ringer's solution was infused into the left femoral vein at a rate of 17 ml/kg/min for 60 sec. This infusion induces an immediate increase in cardiac output followed by a plateau.

All hemodynamic variables were monitored for 15 min after volume overload, until all parameters had returned to baseline levels.

5. *Ex vivo* determination of left ventricular pressure–volume curves

Passive pressure–volume characteristics of the left ventricle were defined as previously described by Fletcher *et al.* (9). A saturated potassium chloride solution was introduced directly into the vena cava until the heart had stopped in diastole. The heart was then carefully excised, rinsed, and a cannula was inserted 5 mm into the left ventricle through the ascending aorta. The right and left atrioventricular junctions were ligated as well as the pulmonary artery and vena cava. The left ventricle was compressed manually to expel blood and create a negative pressure, which was taken as zero volume. Physiologic saline was infused at 0.68 ml/min via the cannula while intraventricular pressure was continually recorded over the range of negative pressure to 30 mm Hg. At least two reproducible pressure–volume curves were obtained within the 10 min after cardiac arrest, well before the onset of rigor mortis. Ventricular volumes at pressures of 0, 2.5, 5, 10, 15, 20, and 30 mm Hg were determined from the pressure–volume curves. The operating LVEDV was derived from the left ventricular pressure–volume curve and was defined as the volume on the pressure–volume curve corresponding to a filling pressure equal to *in vivo* end-diastolic pressure.

6. Assessment of infarct size and cardiac geometry 7 days after coronary ligation

After the pressure–volume data had been recorded, the hearts were slowly frozen in liquid nitrogen and cut at –20°C with a cryostat (Leica CM3050 S, Leica Microsystems, Wetzlar, Germany). Six transverse 20- μ m sections were obtained at different levels of the ventricular mass every 1.5 mm from the apex of the heart to the base of the ventricles.

Estimation of cardiac necrosis

Each section was stained using nitroblue tetrazolium (0.04% in 0.05 M sodium succinate buffer, pH 7.6). On each section, necrotic and non-necrotic tissues were distinguished by the absence or presence of staining, respectively, and the estimation of infarct size was evaluated by planimetry. The lengths of necrotic tissue and of noninfarcted muscle for both the endocardial and epicardial surfaces of each histologic section were determined by planimetry of the projected histologic slides. The lengths of scar for the endocardial and

epicardial surfaces for all histologic sections were numerically summed separately, as were the endocardial and epicardial circumferences. The ratio of the sums of the lengths of scar and of surface circumference defined the infarct size for each of the myocardial surfaces. Final infarct size was expressed in a percentage as the average of the infarct sizes of the endocardial and epicardial surfaces \times 100.

Assessment of cardiac geometry

The study regarding cardiac architecture was performed on tissue from one level (5.5 mm from the apex), as described by Sulpice *et al.* (18). For each section, the cross-sectional area of left ventricle cavity (LV cav csa) and the cross-sectional area of the entire left ventricle (LV csa) were measured by using planimetry on all levels for each heart. For each heart, the ratio of LV cav csa/LV csa corresponds to an index of LV-cavity dilation (DI). The thickness of the infarcted wall, septum, and right ventricular wall were measured on cross sections. The thinning index (TI) was defined as the ratio between the thickness of the infarcted wall and that of the septum. Expansion index (EI) was estimated by the ratio DI/TI.

7. Statistical analysis

Results were expressed as mean \pm standard error of the mean (SEM). One-way analysis of variance was performed to determine the presence of significant differences between the various groups. The significance of the difference between the mean of the groups was tested with the *a posteriori* PLSD test of Fisher. A value of $p < 0.05$ was considered as the threshold of statistical significance.

REFERENCES

- Berthonneche C, Sulpice T, Boucher F, Gouraud L, de Leiris J, O'Connor SE, Herbert JM, and Janiak P. New insights into the pathological role of TNF- α in early cardiac dysfunction and subsequent heart failure following myocardial infarction in rats. *Am J Physiol* 287: H340–H350, 2004.
- Berthonneche C, Sulpice T, Tanguy S, O'Connor SE, Herbert J-M, Janiak P, de Leiris J, and Boucher F. AT1 receptor-blockade prevents cardiac dysfunction and remodeling and limits TNF- α generation early after myocardial infarction in rats. *Cardiovasc Drugs Ther* 19: 251–259, 2005.
- Bloch KD and Janssens S. Cardiocyte-specific overexpression of nitric oxide synthase 3: impact on left ventricular function and myocardial infarction. *Trends Cardiovasc Med* 15: 249–253, 2005.
- Brady AJB, Poole-Wilson PA, Harding SE, and Warren JB. Nitric oxide production within cardiac myocytes reduces their contractility in endotoxemia. *Am J Physiol* 263: H1963–H1966, 1992.
- Cooke JP. NO and angiogenesis. *Atheroscler Suppl* 4: 53–60, 2003.
- Dutka DP, Elborn JS, Delamere F, Shale DJ, and Morris GK. Tumor necrosis factor alpha in severe congestive cardiac failure. *Br Heart J* 70: 141–143, 1993.
- Feng Q, Lu X, Jones DL, Shen J, and Arnold JM. Increased inducible nitric oxide synthase expression contributes to myocardial dysfunction and higher mortality after myocardial infarction in mice. *Circulation* 104: 700–704, 2001.
- Finkel MS, Oddis CV, Jacob TD, Watkins SC, Hattler BG, and Simmons RL. Negative inotropic effects of cytokines on the heart mediated by nitric oxide. *Science* 257: 387–389, 1992.
- Fletcher PJ, Pfeffer JM, Pfeffer MA, and Braunwald E. Left ventricular diastolic pressure-volume relations in rats with healed myocardial infarction. *Circ Res* 49: 618–26, 1981.
- Funakoshi H, Kubota T, Machida Y, Kawamura N, Feldman AM, Tsutsui H, Shimokawa H, and Takeshita A. Involvement of inducible nitric oxide synthase in cardiac dysfunction with tumor necrosis factor- α . *Am J Physiol* 282: H2159–H2166, 2002.
- Hou J, Kato H, Cohen RA, Chobanian AV, and Brecher P. Angiotensin II-induced cardiac fibrosis in the rat is increased by chronic inhibition of nitric oxide synthase. *J Clin Invest* 96: 2469–2477, 1995.

12. Kelly RA, Balligand JL, and Smith TW. Nitric oxide and cardiac function. *Circ Res* 79: 363–380, 1996.
13. Kempf T and Wollert KC. Nitric oxide and the enigma of cardiac hypertrophy. *Bioassays* 26: 608–615, 2004.
14. Kim YM, Bombeck CA, and Billiar TR. Nitric oxide as a bifunctional regulator of apoptosis. *Circ Res* 84: 253–256, 1999.
15. Kojda G and Kottenberg K. Regulation of basal myocardial function by NO. *Cardiovasc Res* 41: 514–523, 1999.
16. Krown KA, Page MT, N'Guyen C, Zechner D, Gutierrez V, Comstock KL, Quintana PJE, and Sabbadini RE. Tumor necrosis factor alpha-induced apoptosis in cardiac myocytes: involvement of the sphingolipid signaling cascade in cardiac death. *J Clin Invest* 98: 2854–2865, 1996.
17. Levine B, Kalman J, Mayer L, Fillit HM, and Packer M. Elevated circulating levels of tumor necrosis factor in severe chronic heart failure. *N Engl J Med* 323: 236–241, 1990.
18. Murray DR, Prabhu SD, and Freeman GL. Hemodynamic effects of nitric oxide synthase inhibition at steady state and following tumor necrosis factor-alpha-induced myodepression. *Cardiovasc Res* 44: 527–535, 1999.
19. Rhode LE, Ducharme A, Arroyo LH, Aikawa M, Sukhova G, McClure KF, Mitchell PG, Libby P, and Lee RT. Matrix metalloproteinase inhibition attenuates early left ventricular enlargement after experimental myocardial infarction in mice. *Circulation* 99: 3063–3070, 1999.
20. Saito T, Hu F, Tayara L, Fahas L, Shennib H, and Giaid A. Inhibition of NOS II prevents cardiac dysfunction in myocardial infarction and congestive heart failure. *Am J Physiol* 283: H339–H345, 2002.
21. Satoh M, Nakamura M, Tamura G, Makita S, Segawa I, Tashiro A, Satodate R, and Hiramori K. Inducible nitric oxide synthase and tumor necrosis factor-alpha in myocardium in human dilated cardiomyopathy. *J Am Coll Cardiol* 29: 716–724, 1997.
22. Sugamori T, Ishibashi Y, Shimada T, Takahashi N, Sakane T, Ohata S, Kunizawa Y, Inoue S, Nakamura K, Ohta Y, Shimizu H, Katoh H, Oyake N, Murakami Y, and Hashimoto M. Increased nitric oxide in proportion to the severity of heart failure in patients with dilated cardiomyopathy: close correlation of tumor necrosis factor-alpha with systemic and local production of nitric oxide. *Circ J* 66: 627–632, 2002.
23. Sulpice T, Boucher F, and de Leiris J. Limiting lipid peroxidation in the non ischemic zone of infarcted rat hearts by indomethacin improves left ventricular function without affecting myocardial healing and remodeling. *Am Heart J* 131: 681–688, 1996.
24. Torre-Amione G, Kapadia S, Lee J, Durand JB, Bies RD, Young JB, and Mann DL. Tumor necrosis factor-alpha and tumor necrosis factor receptors in the failing human heart. *Circulation* 93: 704–711, 1996.
25. Wollert KC and Drexler H. Regulation of cardiac remodeling by nitric oxide: focus on cardiac myocyte hypertrophy and apoptosis. *Heart Fail Rev* 7: 317–325, 2002.
26. Yokoyama T, Nakano M, Bednarczyk JL, McIntyre BW, Entman M, and Mann DL. Tumor necrosis factor- α provokes a hypertrophic growth response in adult cardiac myocytes. *Circulation* 95: 1247–1252, 1997.
27. Yokoyama T, Vaca R, and Rossen D. Cellular basis for the negative inotropic effects of tumor necrosis factor-alpha in the adult mammalian cardiac myocyte. *J Clin Invest* 92: 2303–2312, 1993.
28. Zheng B, Cao LS, Zeng QT, Wang X, Li DZ, and Liao YH. Inhibition of NOS2 ameliorates cardiac remodeling, improves heart function after myocardial infarction in rats. *Basic Res Cardiol* 99: 264–271, 2004.

Address reprint requests to:

Pr. François Boucher

Equipe Coeur & Nutrition, Laboratoire TIMC-PRETA

UMR5525-IFRT 130 Ingénierie pour le Vivant

Bâtiment Jean Roget, Domaine de la Merci

Université Joseph Fourier

38706 La Tronche Cedex, France

E-mail: Francois.Boucher@ujf-grenoble.fr

Date of first submission to ARS Central, January 4, 2007; date of acceptance, February 2, 2007.

This article has been cited by:

1. Zita Hertelendi , Attila Tóth , Attila Borbély , Zoltán Galajda , Jolanda van der Velden , Ger J.M. Stienen , István Édes , Zoltán Papp . 2008. Oxidation of Myofilament Protein Sulfhydryl Groups Reduces the Contractile Force and Its Ca²⁺ Sensitivity in Human Cardiomyocytes. *Antioxidants & Redox Signaling* **10**:7, 1175-1184. [[Abstract](#)] [[PDF](#)] [[PDF Plus](#)]
2. F. R. Boucher, M. -G. Jouan, C. Moro, A. N. Rakotovao, S. Tanguy, Joël Leiris. 2008. Does selenium exert cardioprotective effects against oxidative stress in myocardial ischemia?. *Acta Physiologica Hungarica* **95**:2, 187-194. [[CrossRef](#)]